JOURNAL OF SPACECRAFT AND ROCKETS
Vol. 31, No. 1, January–February 1994

Semiactive Vibration Suppression of Truss Structures by Coulomb Friction

Junjiro Onoda* and Kenji Minesugi†
Institute of Space and Astronautical Science, Kanagawa 229, Japan

An approach for semiactive vibration suppression of truss structures by means of dry friction is proposed and evaluated. The present approach employs frictional truss members and adaptively controls the frictional forces according to the vibration condition. Because of the passive nature, the resulting system is always stable and requires neither high speed nor accurate control, and thus, the control system can be very simple. Furthermore, the control is suitable for local implementation. Numerical simulations of truss structures with multiple variable-frictional members show that the present approach overcomes the disadvantages of passive-frictional damping. A vibration suppression experiment demonstrates the practicality of this approach.

Nomenclature

a =initial amplitude of vibration
$[B]$ =$[\{b_1\}, \{b_2\}, \ldots, \{b_{m_a}\}]$
$\{b_i\}$ =vector of influence coefficients for e_i, see Eqs. (14) and (17)
c =amplitude of vibration after a half cycle
$[E]$ =diagonal (EA_i/l_i)
EA_i =longitudinal stiffness of the ith element
e, e_i =frictional slip
$\{e\}$ =vector of frictional slip, $[e_1, e_2, \ldots, e_{m_a}]^T$
$\tilde{e}_i$ =normalized frictional slip of the ith frictional member, $e_i EA_i/(g_{ji} l_i)$
F, F_i =dry frictional force
$\tilde{F}_i$ =normalized dry frictional force of the ith frictional member, $|g_{ji}|F_i l_i/(EA_i)$
$\{f\}$ =nodal force vector in global coordinate, $\Sigma_i\{f_i\}$
$\{f_i\}_L$ =nodal force vector of the ith element in the local coordinate, $[f_{j1}, f_{j2}, f_{j3}, f_{k1}, f_{k2}, f_{k3}]^T$
f_{m_n} =nodal force of the mth node in the nth direction
g_{ji} =jth row, ith column element of $-[\Phi]^T[B]$
$[K]$ =stiffness matrix of entire system in global coordinate, $\Sigma_i[K_i]$
$[K_i]$ =stiffness matrix of the ith element in global coordinate
k_1, k_2 =spring constants, see Fig. 1
$\tilde{k}_1$ =normalized spring constant, $\omega_j^2 - \tilde{k}_2$
$\tilde{k}_{2i}$ =normalized spring constant of the ith frictional member, $g_{ji}^2 f_i/(EA_i)$
$\tilde{k}_2$ =normalized spring constant, $\Sigma_i \tilde{k}_{2i}$
l_i =length of the ith element
$[M]$ =mass matrix in the global coordinate
m_a =total number of frictional members
p =force transferred through the friction
$\{p\}$ =vector of loads on the frictional members, $[p_1, p_2, \ldots, p_{m_a}]^T$
p_i = axial load on the ith frictional member
$\{p_0\}$ =$-[B]^T[\Phi]\{q\}$
p_{0i} =ith element of $\{p_0\}$
$\{q\}$ =displacement vector in modal coordinate
r_h^2 =energy reduction factor per half cycle
T =control interval
$[T_i]$ =transformation matrix from the ith local coordinates to the global coordinates
u =displacement of mass, see Fig. 1
$\{u_i\}_L$ =nodal displacement vector of the ith element in the local coordinate, $[u_{j1}, u_{j2}, u_{j3}, u_{k1}, u_{k2}, u_{k3}]^T$
u_{m_n} =displacement of the mth node in the nth direction
u_{rms} =root-mean-square displacement
V =input voltage to piezoelectric actuator
β =ak_2/F
γ =$\Delta e k_2/(2F)$
γ_i =$\Delta e_i EA_i/(2F_i l_i)$
γ_{opt} =optimal value of γ read from Fig. 3
Δe =amount of frictional slip (i.e., the difference between the maximum and minimum values of e) during a half cycle, $\Delta e \geq 0$
Δp =variation (i.e. the difference between the maximum and minimum values) of p during a half cycle, $\Delta p \geq 0$
δ_{ij} =Kronecker delta function
ζ =effective damping rate, $-\ln(r_h)/\omega\tau_h$
κ =stiffness ratio, k_2/k_1
λ_i =$1/\gamma_i$
λ_{Ti} =target value for λ_i
μ =small positive constant
τ_h =half-cycle period
$[\Phi]$ =$[\{\phi_1\}, \{\phi_2\}, \ldots, \{\phi_n\}]$
$\{\phi_i\}$ =modal shape of the ith mode without any frictional slip
$[\Omega]$ =diagonal (ω_i^2)
ω =natural angular frequency of single-degree-of-freedom system shown in Fig. 1 without any frictional slip, $\sqrt{(k_2+k_1)/m}$
ω_i =natural angular frequency of the ith mode of the structure without any frictional slip

Subscript
L = local coordinate

Introduction

VIBRATION suppression of space structures is an important and difficult problem because in many cases their damping is expected to be small whereas the operational requirement for the tolerable vibration level and the transient vibration is stringent. An attractive approach for the problem is active vibration suppression. Numerous works have been published on the subject with various types of actuators. One of the most attractive actuators for active vibration suppression of truss structures is the variable-length truss member, which elongates and contracts, thus generating an internal force in the process. Particularly, the variable-length active members that are composed of piezoelectric actuators have been extensively studied because of their simplicity, light weight, and

Received March 9, 1992; presented as Paper 92-2270 at the 32nd AIAA/ASME/ASCE/AHS/ASC Structures, Structural Dynamics, and Materials Conference, Dallas, TX, April 13–15, 1992; revision received Dec. 2, 1992; accepted for publication Dec. 3, 1992.

*Professor. Member AIAA.
†Research Associate.

minimum consumption of source power.[1,2] Although this approach is excellent, it may trigger a spillover instability when the control logic is improper or the mathematical model employed for control is not adequate enough due to the difficulty in identification of space structures. In addition, the very short stroke length of piezoelectric members may be an inherent limiting factor in many applications.

An alternative approach is passive vibration suppression,[3,4] with which the system is always stable, although the damping rate is relatively slow. Among the passive approaches, vibration suppression with dry frictional mechanisms can conceptually offer several advantages such as robustness, and lightweight hardware. In a previous study,[5] the use of dry frictional mechanisms resulted in reducing the power spectral density of vibration of a 10-kg battery on a Japanese scientific satellite by 25 dB with a penalty of less than 1-g mass increment, thus demonstrating its weight efficiency. In the case of truss structures, a possible implementation for creating dry frictional force is to use telescopic members which can be elongated and contracted. However, it also has several disadvantages. When the amplitude of frictional force is small, so is its damping amount. If the frictional force is large, the vibration damps rapidly as long as the frictional surfaces continue to slip. However, the surfaces cease to slip when the vibration amplitude decreases below a certain level, and thus friction no longer contributes to the vibration suppression. In addition, static deformation remains if the slip stops at a location other than the neutral position. Another concern is the possible variation of the frictional coefficients due to the variation of slip surface condition.

In this paper, we propose a semiactive vibration suppression, which combines the advantageous features of both the active control and passive damping. In so doing we will build upon the experience we obtained during the course of the development of variable-stiffness truss members.[6] Specifically, in lieu of the variable-stiffness strategy,[6] we rely on an active control system to adjust the frictional force according to the observed condition of the vibrational motions whereas the actual dissipative functions are realized by dry friction mechanisms. The result is a semiactive vibration suppression system, which is always stable, at least in the sense of Lyapunov, because the frictional element cannot supply energy to the system. Therefore, there will be no spillover instability, and the control system can be very simple. Even when the conditions of the slip surfaces (i.e., the frictional coefficients) vary, the frictional force will be adjusted by the control system. Therefore, the present approach appears to be attractive when robustness is an overriding concern. It seems to overcome the mentioned disadvantages while keeping the advantages by introducing a primitive control.

Damping Characteristics of a Single-Degree-of-Freedom System with Dry Friction

To study the damping characteristics of systems with dry friction, let us first investigate the simple system shown in Fig. 1. For simplicity, we assume that the static and dynamic frictional forces are identical with each other. As will be shown later, this model represents the behavior of a single vibration mode of structures with frictional elements. Because of the spring k_2, this system is different from the basic single-degree-of-freedom (SDOF) system with dry friction shown in most text books. The slip displacement

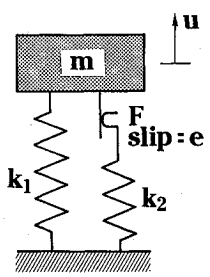

Fig. 1 Single-degree-of-freedom system with dry friction.

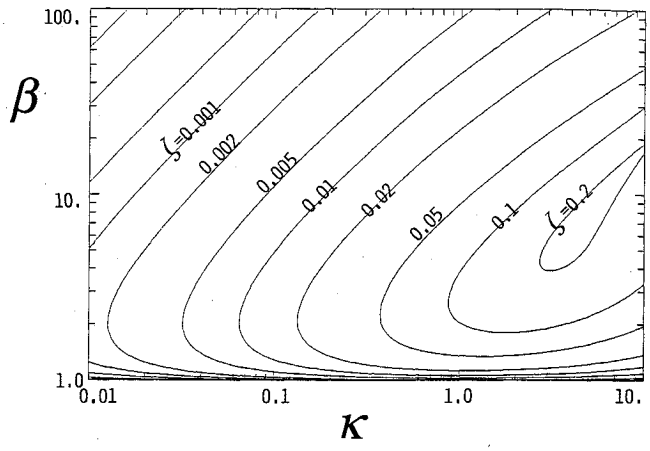

Fig. 2 Effective damping rate of single-degree-of-freedom system as a function of β and κ.

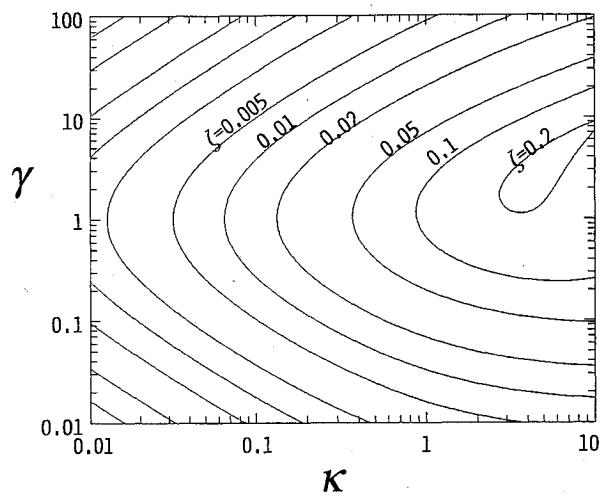

Fig. 3 Effective damping rate of single-degree-of-freedom system as a function of γ and κ.

e is introduced in addition to u to describe the state. The force p transferred to the mass through the friction is equal to the load on the spring k_2 as

$$p = k_2(u-e) \tag{1}$$

If the external force is zero, the equation of motion of this system is

$$m\ddot{u} + k_1 u + k_2(u-e) = 0 \tag{2}$$

When the absolute value of p is about to exceed F, the frictional slip starts and the value of e follows the variation of u as

$$\begin{aligned} \dot{e} &= \dot{u} \text{ when } F \le k_2(u-e) \text{ and } 0 < \dot{u} \\ &= \dot{u} \text{ when } -F \ge k_2(u-e) \text{ and } 0 > \dot{u} \\ &= 0 \text{ otherwise} \end{aligned} \tag{3}$$

To obtain the damping rate of this system, let us investigate the half cycle when the mass has been moving toward the positive direction causing frictional slip and then stops at the point $u = a$. The initial conditions for this half cycle are

$$u = a \tag{4a}$$

$$\dot{u} = 0 \tag{4b}$$

$$p = F \tag{4c}$$

As shown in the Appendix, the energy of the system reduces by the factor of r_h^2 during the half-cycle period τ_h, if

$$a > F/k_2 \tag{5}$$

where

$$r_h^2 = \frac{\kappa^2\left[1-\sqrt{1+(4/\kappa)+(\beta/\kappa)^2-(2\beta/\kappa)}\right]^2+\kappa}{\kappa+\beta^2} \tag{6}$$

$$\tau_h = \omega^{-1}\left(\cos^{-1}\left[\frac{\beta-2-\kappa}{\kappa+\beta}\right]+\sqrt{1+\kappa}\,\tan^{-1}\left[\frac{2\sqrt{\beta-1}}{2+\kappa-\beta}\right]\right) \tag{7}$$

Otherwise, the energy does not reduce at all. The value of effective damping rate ζ can be numerically calculated as shown in Fig. 2.

Semiactive Vibration Suppression of Single-Degree-of-Freedom Systems

Figure 2 indicates that there is an optimal value of β which maximizes the damping rate for each given value of κ. This fact, together with the definition of β, means that there is an optimal value of F according to the vibration amplitude a. The figure also shows that the vibration ceases to damp when it is suppressed to the level of $\beta=1$ (i.e., $a=F/k_2$), and as a result, the amplitude of residual vibration remains. The figure suggests that a promising approach to obtain the maximum damping and to overcome the disadvantage of the residual vibration is to control the value of F according to the vibration amplitude such that the value of β is optimal.

To implement this semiactive control, the values of F and a have to be known. Direct measurements of these variables may not always be easy, especially when u represents a modal displacement as will be shown later in an example in this paper. It is convenient if we can control F by monitoring variables that can be easily and locally measured at the frictional element, especially for decentralized control. For this purpose, let us seek another approach by introducing another parameter γ which is defined as $\Delta e k_2/(2F)$.

When Eq. (5) is held, the amount of frictional slip during the half cycle Δe can be estimated as

$$\Delta e = a - c - 2F/k_2 \tag{8}$$

(see Appendix) where c is given by Eq. (A11). By using Eq. (8), the damping characteristics of the system can be resummarized in the term of γ instead of β as shown in Fig. 3 The figure shows that there also is an optimal value for γ. When Eq. (5) is satisfied, the value of p varies from F to $-F$ during the half cycle as shown in the Appendix, resulting in

$$2F = \Delta p \tag{9}$$

As a result, the value of γ can be estimated as

$$\gamma = \Delta e k_2/\Delta p \tag{10}$$

Therefore, when Eq. (5) is satisfied, an alternative approach is to control F such that the value of γ is optimal by monitoring Δe and Δp. It is clear that the normal force for friction should be increased when γ is too large and should be decreased when γ is too small.

When Eq. (5) is not satisfied, the value of γ estimated from Eq. (10) is zero because no slip occurs (i.e., $\Delta e=0$). If the mentioned control is applied to this case, the control logic decreases F, making the system satisfy Eq. (5). Consequently, this control logic can be expected to work well even when Eq. (5) is not satisfied.

Because p and e can be measured easily and locally, this approach can be easily implemented. Figure 3 also shows that neither the increment by twice nor decrement by half of the value of γ results in a drastic degradation of the damping, suggesting that very high accuracy is not required for control. Because F is reduced to a small level by this control logic when the vibration has been reduced to a low level, no substantial static displacement will remain after the completion of vibration suppression.

Equations of Motion of Truss Structures with Frictional Members

To investigate the application of the semiactive approach introduced in the preceding section to the truss structures, let us first formulate the equations of motion of the truss with frictional members. We assume that the truss structure involves some frictional members, which elongate or contract due to the frictional slip when it is pulled or compressed, respectively, by a larger force than the dry frictional force. Let us model each truss member by a bar finite element and define the local coordinates, nodal forces, and displacements of the frictional members as shown in Fig. 4. The relation between the load in the ith frictional element and the nodal displacements is

$$p_i = (EA_i/l_i)\,(u_{k1} - u_{j1} - e_i) \tag{11}$$

The characteristics of the ith element can be described as

$$\{f_i\}_L = [K_i]_L\{u_i\}_L + \{b_i\}_L e_i \tag{12}$$

where

$$[K_i]_L = \frac{EA_i}{l_i}\begin{bmatrix} 1 & 0 & 0 & -1 & 0 & 0 \\ 0 & 0 & 0 & 0 & 0 & 0 \\ 0 & 0 & 0 & 0 & 0 & 0 \\ -1 & 0 & 0 & 1 & 0 & 0 \\ 0 & 0 & 0 & 0 & 0 & 0 \\ 0 & 0 & 0 & 0 & 0 & 0 \end{bmatrix} \tag{13}$$

$$\{b_i\}_L = \frac{EA_i}{l_i}[1, 0, 0, -1, 0, 0]^T \tag{14}$$

Equation (12) can be translated into global coordinates as follows:

$$\{f_i\} = [K_i]\{u\} + \{b_i\}e_i \tag{15}$$

where

$$[K_i] = [T_i]\,[K_i]_L\,[T_i]^T \tag{16}$$

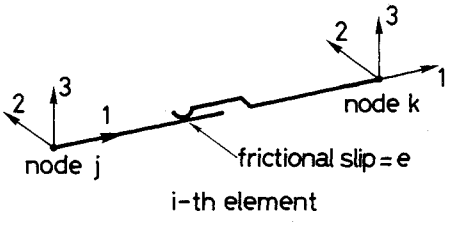

Fig. 4 Bar finite element with frictional slip.

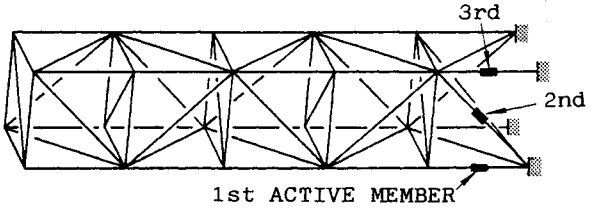

Fig. 5 Cantilevered truss beam with frictional members.

Table 1 Values of $\tilde{k}_2/\tilde{k}_1$ of the example truss for each mode

Mode	1	2	3	4	5	6	7	8	9	10
$\tilde{k}_2/\tilde{k}_1$	0.420	0.245	0.103	0.104	0.049	0.188	0.078	0.026	0.124	0.029

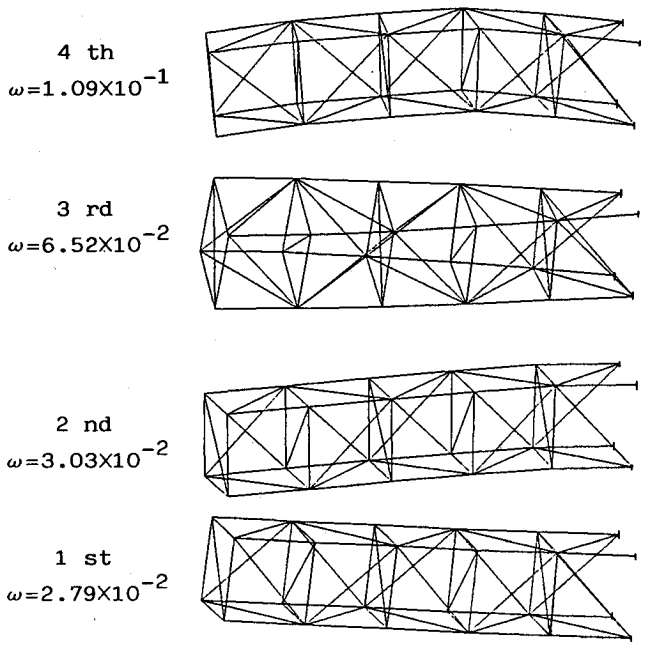

Fig. 6 Natural frequencies and vibration modes of cantilevered truss beam.

$$\{b_i\} = [T_i]\{b_i\}_L \tag{17}$$

By assembling these element matrices, including the nonfrictional ones, into those of the total system, the following equation can be obtained:

$$\{f\} = [K]\{u\} + [B]\{e\} \tag{18}$$

Thus, when the external force is zero, the equation of motion of the total system is

$$[M]\{\ddot{u}\} + [K]\{u\} + [B]\{e\} = 0 \tag{19}$$

This equation can be translated into the modal coordinates as follows:

$$\{\ddot{q}\} + [\Omega]\{q\} = -[\Phi]^T[B]\{e\} \tag{20}$$

where

$$\{u\} = [\Phi]\{q\} \tag{21}$$

and Φ is normalized such that

$$[\Phi]^T[M][\Phi] = [I] \tag{22}$$

From Eqs. (11), (14), and the definition of $[T_i]$, the load on the ith frictional element can be obtained as

$$p_i = -\{b_i\}_L^T[T_i]^T\{u\} - e_i(EA_i/l_i) \tag{23}$$

Therefore, from Eqs. (17), (21), and (23), the vector of loads on the frictional elements can be described as follows:

$$\{p\} = \{p_0\} - [E]\{e\} \tag{24}$$

When the absolute value of p_i is about to exceed the frictional force F_i of the ith member, the frictional slip starts in the ith member. If $p_i \geq F_i$ and $\dot{p}_{0i} > 0$ or $p_i \leq -F_i$ and $\dot{p}_{0i} < 0$, then the frictional slip occurs in the ith member, and the absolute value of p_i remains at F_i. Therefore, e_i behaves as

$$\begin{aligned} \dot{e}_i &= \dot{p}_{0i}l_i/EA_i \text{ when } F_i \leq p_i \text{ and } 0 < \dot{p}_{0i} \\ &= \dot{p}_{0i}l_i/EA_i \text{ when } -F_i \geq p_i \text{ and } 0 > \dot{p}_{0i} \\ &= 0 \text{ otherwise} \end{aligned} \tag{25}$$

As a result, Eqs. (20), (24), and (25) compose a complete set of equations of motion for a truss structure with frictional members.

Semiactive Vibration Suppression of Truss Structures

The equations of motion of the truss structures in modal coordinates which have been derived in the preceding section show some coupling between the modes through the term of $\{e\}$. However, let us now neglect the coupling and consider only a single mode, e.g., jth mode, to estimate the order of the optimal values for F_i. Equations (20) and (25) can be rewritten, using Eq. (24), as

$$\ddot{q}_j + \omega_j^2 q_j - \sum_i g_{ji}e_i = 0 \tag{26}$$

$$\begin{aligned} \dot{e}_i &= \frac{\dot{q}_j g_{ji} l_i}{EA_i} \text{ when } F_i \leq g_{ji}q_j - \frac{e_i EA_i}{l_i} \text{ and } 0 < g_{ji}\dot{q}_j \\ &= \frac{\dot{q}_j g_{ji} l_i}{EA_i} \text{ when } -F_i \geq g_{ji}q_j - \frac{e_i EA_i}{l_i} \text{ and } 0 > g_{ji}\dot{q}_j \\ &= 0 \text{ otherwise} \end{aligned} \tag{27}$$

Now consider the special case where all the frictional members start and stop slipping synchronously by assuming the following relation for all of the frictional members:

$$\tilde{F}_i = \alpha \tilde{k}_{2i} \tag{28}$$

where α is a constant. Then Eqs. (26) and (27) can be rewritten as

$$\ddot{q}_j + (\tilde{k}_1 + \tilde{k}_2)q_j - \sum_i \tilde{k}_{2i}\tilde{e}_i = 0 \tag{29}$$

$$\begin{aligned} \dot{\tilde{e}}_i &= \dot{q}_j \text{ when } \alpha \leq (q_j - \tilde{e}_i) \text{ and } 0 < \dot{q}_j \\ &= \dot{q}_j \text{ when } -\alpha \geq (q_j - \tilde{e}_i) \text{ and } 0 > \dot{q}_j \\ &= 0 \text{ otherwise} \end{aligned} \tag{30}$$

Because Eq. (30) is identical for all i, we can select the origin of e_i such that

$$\tilde{e}_1 = \tilde{e}_2 = \cdots = \tilde{e}_i = \cdots = \tilde{e}_{m_a} \tag{31}$$

without losing any generality. This allows the equations of motion to be further rewritten as

$$\ddot{q}_j + \tilde{k}_1 q_j - \tilde{k}_2(q_j - \tilde{e}) = 0 \tag{32}$$

$$\begin{aligned} \dot{\tilde{e}} &= \dot{q}_j \text{ when } \tilde{F} \leq \tilde{k}_2(q_j - \tilde{e}) \text{ and } 0 < \dot{q}_j \\ &= \dot{q}_j \text{ when } -\tilde{F} \geq \tilde{k}_2(q_j - \tilde{e}) \text{ and } 0 > \dot{q}_j \\ &= 0 \text{ otherwise} \end{aligned} \tag{33}$$

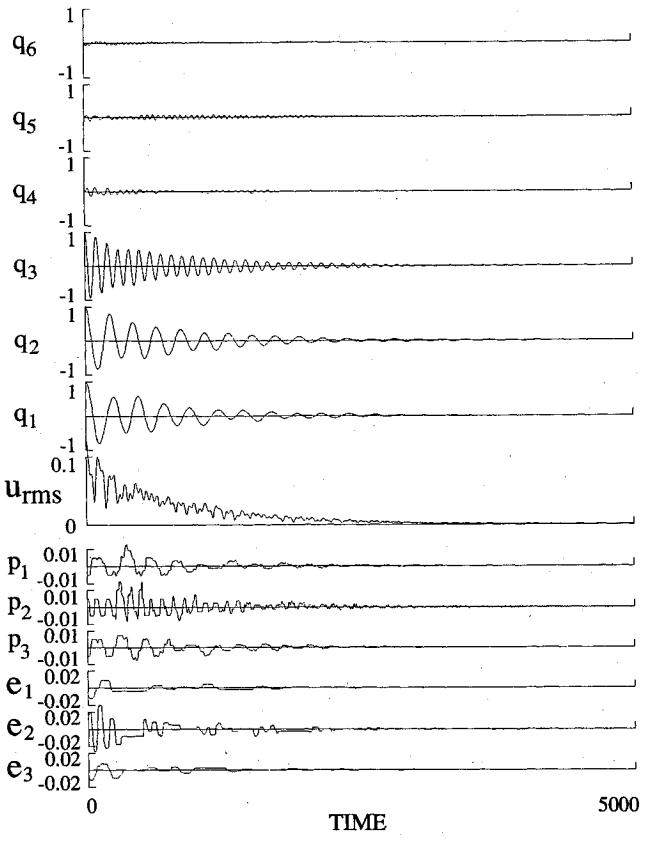

Fig. 7 Simulation result of semiactive vibration suppression, $\lambda_{Ti} = 1/\gamma_{opt}=1.0$.

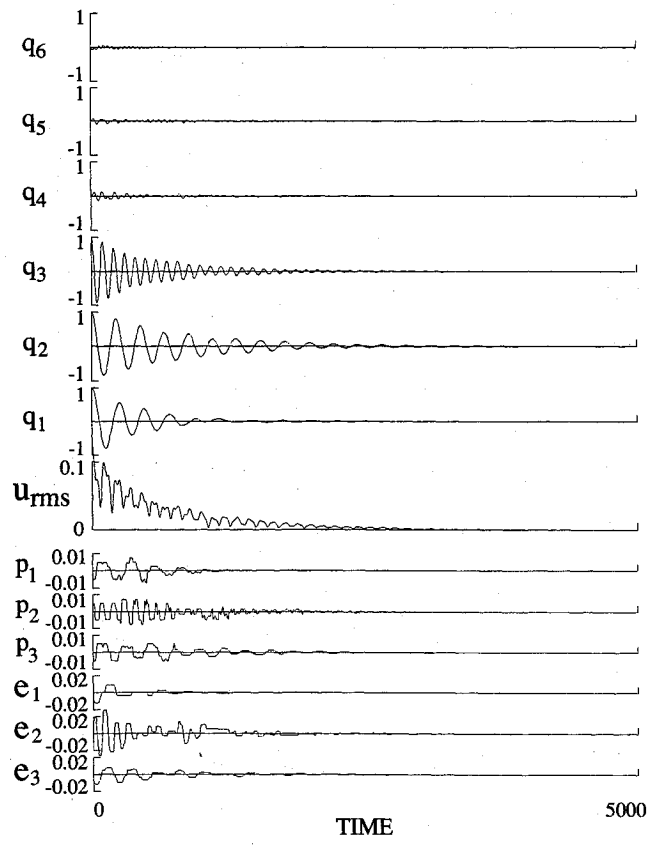

Fig. 8 Simulation result of semiactive vibration suppression, $\lambda_{Ti}=0.5/\gamma_{opt}=0.5$.

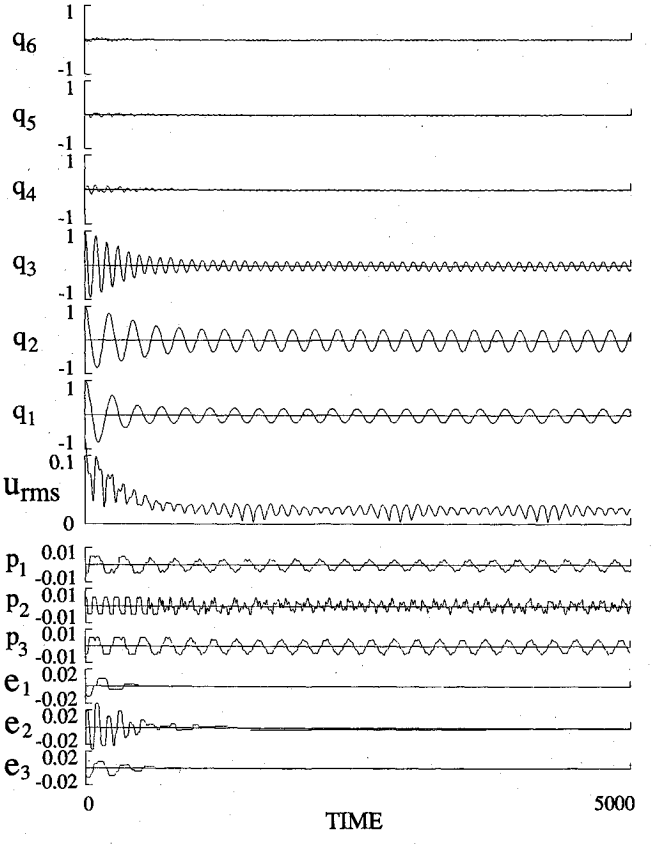

Fig. 9 Simulation result of transient response of truss with dry friction, $F_1=F_2=F_3=0.005$.

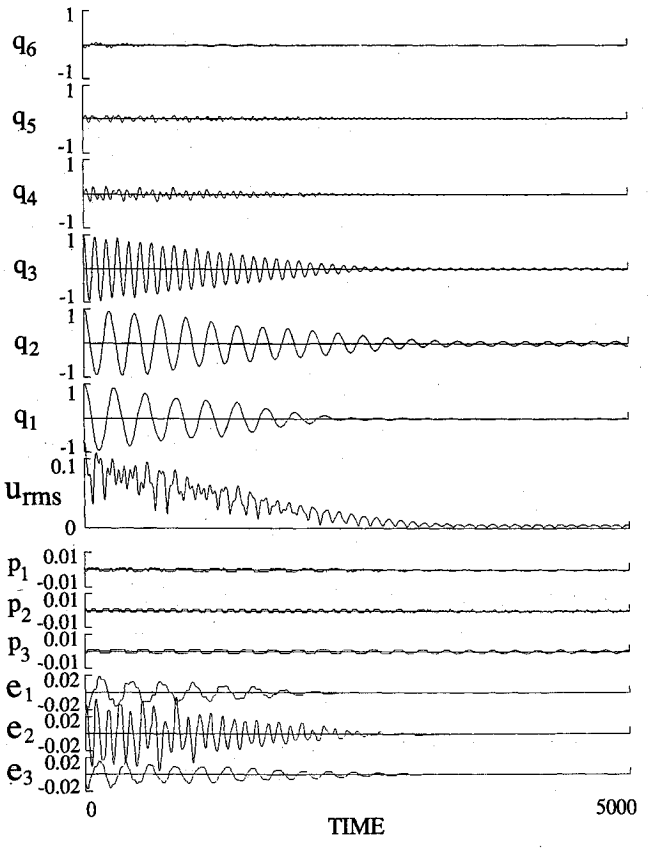

Fig. 10 Simulation result of transient response of truss with dry friction, $F_1=F_2=F_3=0.001$.

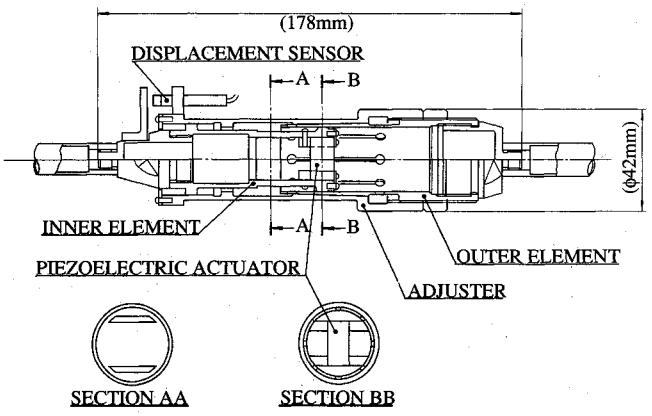

Fig. 11 Construction of variable-friction truss member.

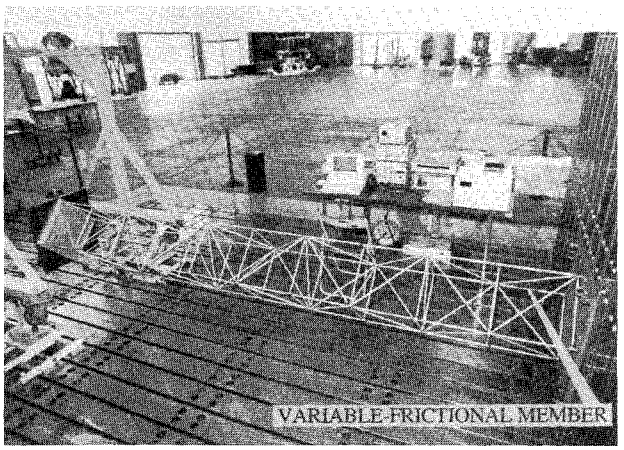

Fig. 12 Truss beam structure with a variable-friction member.

where

$$\tilde{e} \equiv \tilde{e}_1 = \tilde{e}_2 = \cdots = \tilde{e}_i = \cdots = \tilde{e}_{m_a} \tag{34}$$

$$\tilde{F} \equiv \alpha \tilde{k}_2 \tag{35}$$

Because Eqs. (32) and (33) are of the same form as Eqs. (2) and (3), it can be seen from the analogy of these equations that the optimal value of $\Delta \tilde{e} \tilde{k}_2/(2\tilde{F})$ can be roughly estimated from Fig. 3. Furthermore, since the relation

$$\gamma_i \equiv \Delta e_i EA_i/(2F_i l_i) = \Delta \tilde{e} \tilde{k}_2/(2\tilde{F}) \tag{36}$$

can be derived for all i from Eqs. (28), (34), and (35), and $2F_i$ can be estimated as Δp_i, we can see that the friction of the ith frictional member should be controlled such that

$$\Delta e_i EA_i/(\Delta p_i l_i) = \gamma_{\text{opt}} \tag{37}$$

where γ_{opt} denotes the optimal value read from Fig. 3 for the case of $\kappa = \tilde{k}_2/\tilde{k}_1$.

This investigation is limited to a special case due to the assumption made in Eq. (28) and by the elimination of coupling between modes. Thus, it should be noted that the obtained target value for the control is only a rough estimation for the general cases. But it may be used as an initial guess value in many situations.

Numerical Simulation of Semiactive Vibration Suppression of Truss Structures

As an example, the vibration of the truss shown in Fig. 5 is investigated. The length of the members is unity except for the diagonal ones. The stiffness and mass per unit length of the members are also unity, and the inherent damping is zero. Three frictional members are installed so that all of the vibration modes can be suppressed. It should be noted that the truss is stable even when all of these frictional members are removed, because of the additional member in the bottom bay. Figure 6 shows the lowest four vibration modes of the truss. The third mode is torsional whereas the others are bending modes. The values of $\tilde{k}_2/\tilde{k}_1$ for the lowest 10 modes of this structure are less than 0.5 as shown in Table 1. From Fig. 3, the optimal value for $\Delta e_i EA_i/(\Delta p_i l_i)$, i.e., γ_{opt}, can be roughly estimated as 1.0 for all modes.

In the numerical simulation, the values of p_i and e_i of each frictional member are monitored for approximately a cycle period of the lowest vibration mode, and then the maximum and minimum values of them are obtained, and the inverse value of γ_i is estimated for each frictional member as

$$\lambda_i \equiv 1/\gamma_i = (p_{i_{\max}} - p_{i_{\min}})\, l_i / \left[(e_{i_{\max}} - e_{i_{\min}} + \mu)\, EA_i\right] \tag{38}$$

Then the value of λ_i is compared with the target value λ_{Ti}, and the value of F_i is varied as

$$\begin{aligned}
&\text{if} \quad \lambda_{Ti} < \lambda_i < 2\lambda_{Ti}, \text{ decrease } F_i \text{ by a factor of } 1/1.5 \\
&\text{if} \quad 2\lambda_{Ti} \le \lambda_i, \text{ decrease } F_i \text{ by a factor of } 1/3.0 \\
&\text{if} \quad \lambda_{Ti} > \lambda_i/\lambda_{Ti} > 2, \text{ increase } F_i \text{ by a factor of } 1.5 \\
&\text{if} \quad \lambda_{Ti}/2 \le \lambda_i, \text{ increase } F_i \text{ by a factor of } 3.0
\end{aligned} \tag{39}$$

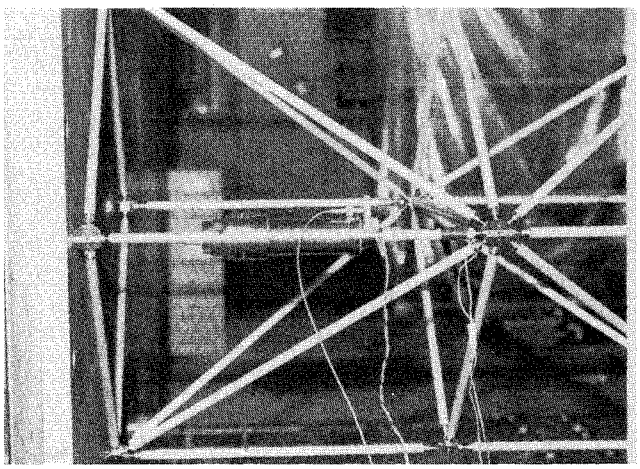

Fig. 13 Variable-friction truss member installed in the truss beam.

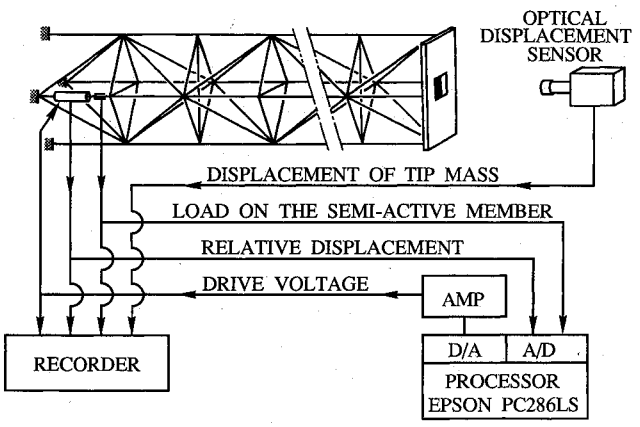

Fig. 14 Block diagram of experiment setup.

The investigation in the preceding section suggests that the target value λ_{Ti} should be approximately $1/\gamma_{opt}$. The small positive value μ in Eq. (38) is introduced to avoid the zero division in the processor and to make the frictional force maximum (i.e., to clamp the slip surface of the frictional member to make the structure stiff) when the vibration has been damped out. For this reason, λ_i is used in the control logic instead of γ_i. The value of μ should be selected reflecting the actual noise level.

Figures 7–10 show the results of some numerical simulations in which the mathematical model has the lowest 10 modes. No damping is assumed except for the controlled friction. The initial conditions are

$$q_1=q_2=q_3=1,\ q_i=0 \quad \text{for} \quad i\geq 4$$

$$\dot{q}_i=0 \text{ for all } i$$

$$F_1=F_2=F_3=0.005$$

Figure 7 shows the case where the values of λ_{Ti} are $1/\gamma_{opt}$ (i.e., 1.0). The figure shows that the lowest three modes, whose initial values are not zero, damp relatively quickly. The higher modes, whose initial values are zero, are excited a little by the coupling terms but then damp out quickly. The time histories of e and p show well-balanced variation of them. Relatively slow damping of the fifth mode coincides with the relatively low value of $\bar{k}_2/\bar{k}_1$ shown in Table 1. The diagonal active member, i.e., the second one, responds mainly to the torsional third mode. The time history of u_{rms} indicates that the vibration amplitudes of higher modes, which are not shown in the figure, are not so large as to affect the shape accuracy of the structure. As has been mentioned, the structure has its own rigidity even when all the frictional forces are zero. In addition, the frictional force is reduced to a very low level in the final phase of suppression and thus no substantial static distortion is left, as shown in the figure.

Figure 8 shows the simulation results whose parameters are identical with those of Fig. 7 except that the values of λ_{Ti} are $0.5/\gamma_{opt}$ (i.e., 0.5). A slightly better damping is seen in Fig. 8 than Fig. 7, suggesting that the actual optimal values of λ are less than the value read from Fig. 3.

Figure 9 shows the results where all of the initial values are the same as those of Fig. 7, but the frictional forces are kept constant (0.005). The figure shows that the vibrations damp in the initial phase. However, when they have damped to a certain level, they do not damp any more and residual vibrations remain. Figure 10 shows the case where the frictional forces are constant at 0.001. The figure indicates that the amplitudes of residual vibrations are small when the frictional forces are small, although the damping rate is slow. A comparison of Figs. 9 and 10 with Figs. 7 and 8 clearly indicates the advantage of the present semiactive control.

Experiment

To confirm the practicality of this approach, an experiment was performed. Figure 11 shows the construction of the variable-frictional truss member which was used in the experiment. A piezoelectric actuator is installed inside the inner element of the telescopic variable-length member. When the compressively

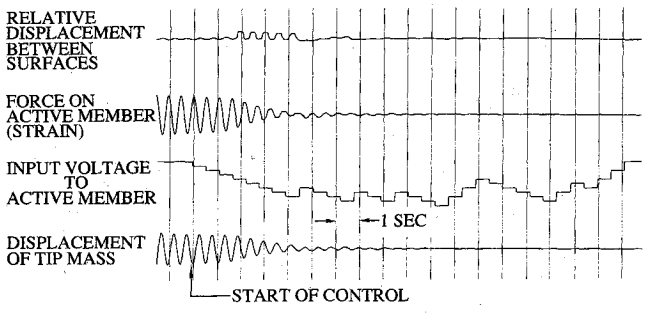

Fig. 15 Example of semiactive vibration suppression.

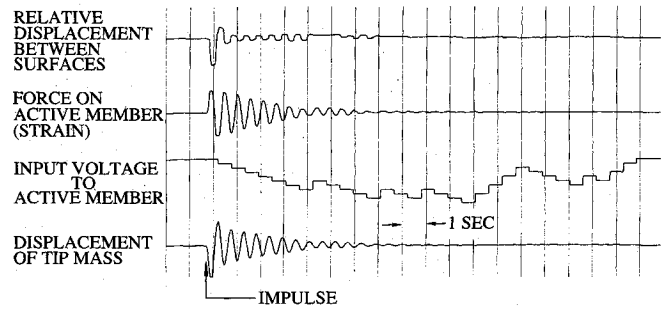

Fig. 16 Response of semiactively controlled truss structure.

preloaded piezoelectric actuator contracts, the normal force between the outer and inner elements decreases, which then decreases the frictional force. When the piezoelectric actuator elongates, the normal force for friction increases, and thus the frictional force increases. The amplitude of the frictional force is a monotonically increasing function of the elongation, i.e., the applied voltage to the piezoelectric actuator. This active truss member was originally fabricated as a variable-stiffness truss member for vibration suppression by stiffness control.[6] An Eddy-current type displacement sensor was also installed for this experiment to measure the amount of slip (or relative displacement between the outer and inner elements). Because the purpose of the experiment is to confirm the concept, weight saving and compactness of the frictional member are not intended.

A cantilevered, 10-bay truss beam with the variable-frictional member at the root was constructed as shown in Figs. 12 and 13. Each bay is 373 mm long. All of the truss members are aluminum tubes whose diameter is 10 mm with a thickness of 1 mm. A mass of 100 kg is attached at the tip of the beam. Since the tip mass is hung by a wire to compensate for gravity, the motion of the tip mass is limited to the horizontal plane. The first mode frequency is 1.9 Hz when the variable-frictional member is clamped, and it decreases to 1.5 Hz when the variable-frictional member is freed or removed. It should be noted that the truss structure is not a mechanism even without the active member, which is a necessary condition to eliminate the static deformation after the complete suppression of vibration.

Figure 14 shows a block diagram of the experiment setup. The strain of the active member (which represents the load p_1) and the relative displacement between the inner and outer elements of the active member (which represents the slip e_1) are fed to the processor. The processor (personal computer EPSON PC-286LS) evaluates the maximum and minimum values of p_1 and e_1 for a duration T, respectively, and then it estimates the value of λ_1 by using Eq. (38). When the value of λ_1 is greater than λ_{T1}, the processor decreases the control voltage V by the amount of ΔV, thereby decreasing the frictional force. Conversely, the control voltage is increased when the value of λ_1 is less than λ_{T1}. In the experiment, the value of λ_{T1} is 1.0. The duration T is approximately the period of the first mode vibration, and ΔV is one-tenth of the input voltage range (i.e., $V_{max}-V_{min}$).

Figure 15 shows an example of the test results. As soon as the control is started while the beam is freely vibrating, the value of V starts decreasing . When the value of V decreases to a certain level, the frictional slip starts and the vibration starts damping. When the amplitude of vibration decreases and the inner and outer elements cease to slip, the control system further decreases the value of V. As a result, the elements start slipping again, and the vibration resumes damping. And finally, the vibration is suppressed to a very low level. In the figure, the time history of the force on the active member shows flat plateaus without any initial spikes when the surfaces slip. This fact suggests that the difference between static and dynamic frictional coefficients are negligible in this case. Figure 16 shows an example where the structure is impulsively excited while the control system is turned on. Even in this case, the present approach suppresses the vibration nicely.

Conclusions

A new approach for semiactive vibration suppression of space truss structures has been proposed and demonstrated. The present approach relies on dry frictional mechanisms for providing attenuation and active control for adaptively adjusting the frictional forces according to the vibration condition. Because of the passive nature, the resulting system is always stable. A simple control logic has been proposed, which can be locally implemented. A simple control law for adjusting the frictional forces has been developed based on the damping characteristics of a single-degree-of-freedom system with dry friction. Numerical simulations for assessing the present approach for multi-degree-of-freedom cases have been performed on a cantilevered truss structure with three variable-frictional members, and the results indicate the effectiveness of the approach for multi-degree-of-freedom systems. Encouraged by the numerical evaluation, an experiment for semiactive vibration suppression of a cantilevered truss with a variable frictional member was performed, which corroborates the effectiveness of the approach in an actual structure. The numerical simulations and the experiment confirm that the present approach overcomes many difficulties associated with the dry friction approach such as the residual vibration, the static deformation, and the possible variation of frictional coefficient, nevertheless still keeping the robustness.

Appendix: Energy Reduction Factor and Half Cycle Duration of Single-Degree-of-Freedom System with Dry Friction

From Eqs. (1), (4a), and (4c), the initial value of e can be calculated as

$$e = a - F/k_2 \tag{A1}$$

In addition, the value of u continues to reduce (i.e., $\dot{u} < 0$) throughout this half cycle. Therefore, it can be seen from Eq. (3) that the frictional slip does not occur [i.e., Eq. (A1) continues to be held] when the condition

$$a - 2F/k_2 \le u \tag{A2}$$

is held. As a result of Eqs. (2) and (A1), the equations of motion can be rewritten as

$$m\ddot{u} + k_1 u + [F - k_2 (a - u)] = 0 \tag{A3}$$

when Eq. (A2) holds. Equation (A3) can be solved, and the value of u can be seen to violate Eq. (A2) only if Eq. (5) holds. This means that the frictional slip occurs in this half cycle, and thus energy dissipates, only when Eq. (5) is held. If Eq. (5) is held, p can become equal to $-F$, and the frictional slip will start at that moment. The displacement, time, and velocity of the mass at that moment can be calculated as

$$u = a - 2F/k_2 \tag{A4}$$

$$\tau_1 = \omega^{-1} \cos^{-1} [(\beta - 2 - \kappa)/(\kappa + \beta)] \tag{A5}$$

$$\dot{u} = -2a\omega \sqrt{(\beta - 1)/(1 + \kappa)}/\beta \tag{A6}$$

respectively. Because the value of e [defined in Eq. (A1)] starts to follow the variation of u at that moment, it can be seen that

$$e = u + F/k_2 \tag{A7}$$

as far as $\dot{u} < 0$ is held. Therefore, from Eqs. (2) and (A7), the equation of motion for the rest of the half cycle can be derived as

$$m\ddot{u} + k_1 u - F = 0 \tag{A8}$$

From Eqs. (A4), (A6) and (A8), the necessary time for $\dot{u}$ to become zero can be calculated as

$$\tau_2 = \omega^{-1} (1 + \kappa)^{1/2} \tan^{-1} [2 (\beta - 1)^{1/2}/(2 + \kappa - \beta)] \tag{A9}$$

As a result, the half-cycle period can be obtained as $\tau_1 + \tau_2$.

The value of c which denotes the value of u at the moment when the mass stops (i.e., at the end of this half cycle) can be calculated from Eqs. (A8) and (A9) and the initial conditions. But it can also be easily calculated as follows: the difference between the initial and the final energies is equal to the energy dissipated by the frictional slip. Because the frictional slip starts at the moment when $u = a - 2F/k_2$ and stops when $u = c$, the stroke of the frictional slip is estimated by Eq. (8) and the following equation is obtained:

$$\left[\frac{k_1}{2}a^2 + \frac{k_2}{2}\left(\frac{F}{k_2}\right)^2\right] - \left[\frac{k_1}{2}c^2 + \frac{k_2}{2}\left(\frac{F}{k_2}\right)^2\right] = \left[a - c - \frac{2F}{k_2}\right]F \tag{A10}$$

By solving this equation, c can be obtained as

$$c = \frac{a\kappa}{\beta}\left[1 - \sqrt{1 + \frac{4}{\kappa} + \left(\frac{\beta}{\kappa}\right)^2 - \frac{2\beta}{\kappa}}\right] \tag{A11}$$

From these results, the energy reduction factor of free decay vibration per half-cycle period $\tau_1 + \tau_2$ can be calculated as Eq. (6). It is obvious that $r_h = 1$ when Eq. (5) is not held, because no slip occurs.

References

[1]Fanson, J. L., Blackswood, G. H., and Chu, C.-C., "Active-Member Control of Precision Structures," AIAA Paper 89-1329, April, 1989.

[2]Preumont, A., Sparavier, M., and Dufour, J., "Application of Piezoelectric Actuators to the Active Damping of a Truss Structure," AIAA Paper 90-0950, April 1990.

[3]Barrett, D. J., "A Design for Improving the Structural Damping Properties of Axial Members," Proc. Damping '89, Wright Aeronautical Labs., West Palm Beach, FL, Feb. 1989.

[4]Davis, L. P., Workman, B. J., Chu, C.-C., and Anderson, E. H., "Design of a D-Strut and Its Application Results in the JPL, MIT, and LARC Test Bed," AIAA Paper 92-2274, April 1992.

[5]Onoda, J., Watanabe, N., Tomoya, S. and Todome, K., "Vibration Suppression of MUSES-A BAT Panel," 32nd Space Science and Technology Joint Conference, Tokyo, Oct. 1988 (in Japanese).

[6]Onoda, J., Endo, T., Tamaoki, H., and Watanabe, N., "Vibration Suppression by Variable-Stiffness Members," *AIAA Journal*, Vol. 29, No. 6, 1991, pp. 977–983.